

## Time series analysis and prediction of climate variables of Southern Java waters using support vector regression

Alfi Satriadi<sup>1\*</sup> , Gentur Handoyo<sup>1</sup> 

<sup>1</sup> Department of Oceanography, Faculty of Fisheries and Marine Science, Universitas Diponegoro, Semarang 50275, Indonesia

\* Corresponding author's e-mail: [satriad\\_as@yahoo.co.id](mailto:satriad_as@yahoo.co.id)

### ABSTRACT

Southern Java Waters contribute significantly to aquatic economy of Indonesia by providing abundant fisheries resources. The understanding of sea state of the waters become a focal point. The aims of this paper are to analyze and to predict time series dataset comprising climate variables such as wind speed, surface temperature (SST), precipitation, and surface pressure of Southern Java waters. The analysis has been done by decomposing the time series dataset to its patterns, trend and seasonality, and calculating the correlation matrix of the dataset. The prediction method employs support vector regression (SVR) algorithm. The performance of the resulted models is computed using mean squared error (MSE). The result shows that wind speed of Southern Java Waters is positively correlated with surface pressure and negatively correlated with SST and total precipitation. The lowest MSE occurs in SST model. Meanwhile, the largest MSE is the total precipitation model. The developed models could be used as prediction tools of climate variables for following years in the Southern Java waters.

**Keywords:** wind speed, sea surface temperature, precipitation, surface pressure, support vector regression.

### INTRODUCTION

As a complex system, atmosphere and ocean interactions play an important role. The impact of this interaction influences all aspects of organisms and their living environment. The most significant aspect is how cold or how warm the environment is. This means that the temperature determines survivability of the organisms [Scrosati, 2020; Iwabuchi and Gosselin, 2019].

Sea surface temperature or SST is one of the important parameters for understanding and monitoring various environmental and climatic conditions. Moreover, SST becomes a primary factor to determine the season of a particular region. The interactions between SST and other parameters are an active research study [Docquier et al., 2023; Singh and Roxy, 2022; Wang, 2019]. One of these parameters is wind speed. These two parameters have negative correlation meaning that high wind speed is associated with low SST. Southern Java waters consist of part

of the large Indian Ocean. To be precise it is located in the south of Java and Bali Islands. The dynamics of climate variable such as SST in this location has been intensively studied [Wijaya et al., 2023; Iskandar et al., 2021; Wirasatriya et al., 2020]. The low SST as the effect of high wind speed is driven by water mass bringing nutrients or feeding ground toward the surface, the displacement of this water mass known as upwelling [Wen et al., 2023; Budiman et al., 2022; Horii et al., 2022]. This explains how physical parameters such as SST and wind speed affect biotic factors in the ocean and in broader aspect the waters play important role for aquatic economy of Indonesia. Other aspects of climate variables include precipitation and surface pressure. Understanding precipitation become important related to incidences of fire and extreme weather [Fanin and Van Der Werf, 2017; Ramadhan et al., 2022; Muhammad and Lubis, 2022]. Moreover, the study of surface pressure related to extreme weather in particular extreme high temperature

has been conducted [Kuswanto and Ningtyas, 2016]. The understanding of sea condition in Southern Java waters become important. Recent studies have explored waters conditions such as wind speed, the sea level, tidal characteristic, SST, and chlorophyll-a [Sofiaty and Putranto, 2020; Nurlatifah et al., 2021; Mutaqin and Ningsih, 2023; Hadi et al., 2020]. Although such conditions have been studied, a considerable knowledge gap persists in understanding the related climate variables in particular wind speed, SST, total precipitation, and surface pressure.

Support vector machine (SVM) is widely employed for classification problem. As an extension of SVM for regression problem, SVR is a machine learning algorithm which is a regression model for single output prediction. It introduced by Vapnik and Ducker et al. [Vapnik, 2013; Drucker et al., 1996]. SVR has applied to various real world time series problems such as stock prediction, water resources, and infectious diseases [Dash et al., 2023; Parbat and Chakraborty, 2020; Feng et al., 2020]. Although the SVR model has been examined for the various time series problems, further research is needed for applying SVR model to predict climate variables especially in Southern Java waters.

To address the limitations discussed in two previous paragraphs, this paper aims to examine the relationship between climate variables such as wind speed, SST, precipitation, and surface pressure in southern Java waters. Also, the paper considers their analysis and prediction using SVR. The research outline includes data collection, data preprocessing, trend and seasonal analysis, computation of correlation matrix, and data prediction using SVR algorithm.

## METHODS

The data used in this paper are collected from the European Centre for Medium-range Weather Forecast (ECMWF), specifically from the Copernicus Climate Data Store. The dataset is from ERA5 which is the fifth generation of ECMWF reanalysis climate data [Hersbach et al., 2020]. The dataset consists of spatial and temporal features. The spatial feature of the dataset is the coordinate of the data point starting from 105 to 115.5 degrees East and from 6 to 12 degrees South with 0.25 degrees resolution. This range of coordinates includes Java Island, Bali Island, and the Indian Ocean. The next feature of the dataset is a 6-hourly data step with the range of dataset temporarily from 2013 to 2022. In the stage of processing and postprocessing of the dataset, we use NumPy, Matplotlib, Xarray, and Cartopy [Harris et al., 2020; Hunter, 2007; Hoyer and Hamman, 2017; Met Office, 2010].

Figure 1 depicts the spatial location of the research area of interest. There are four cross-marked points where the influence of wind speed over SST is considered. The coordinates of these points or location are stated in Table 1. The reason behind the chosen four locations is to study the dynamics of SST with respect to wind speed in different settings such as near a strait, in coastal waters, and in the deep waters.

The dataset contains SST and two 10 meters wind velocity components. The wind velocity components include horizontal velocity or  $u$  velocity components and vertical velocity or  $v$  velocity components. All of climate variables exist not only spatially but also temporarily meaning that in a particular coordinate, for example 110

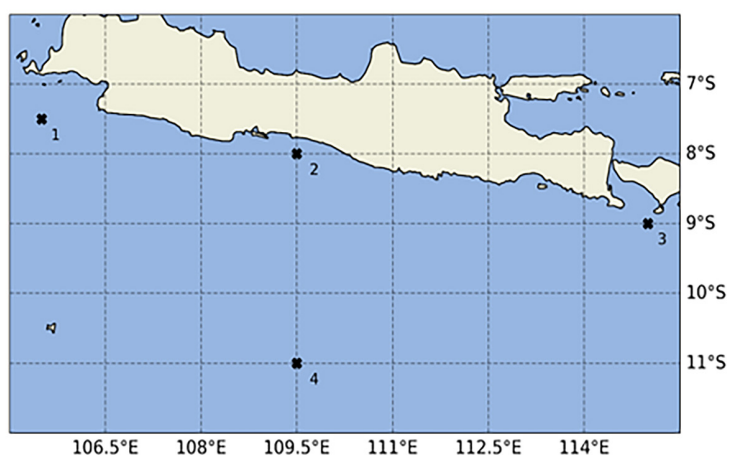


**Figure 1.** The location of the dataset

**Table 1.** The coordinate of the location of data points

Data points	Longitude	Latitude
Location 1	105.5°E	7.5°S
Location 2	109.5°E	8°S
Location 3	115°E	9°S
Location 4	109.5°E	11°S

degrees East and 8 degrees South, there are many data over some range of time. The wind speed is calculated from horizontal and vertical component using following equation:

$$W_s = \sqrt{u^2 + v^2} \quad (1)$$

where:  $W_s$  is the wind speed,  $u$  is the horizontal velocity component, and  $v$  is the vertical velocity component. The unit of wind speed in Equation 1 is in meters per second. Both the dataset variables are resampled from 6-hourly data into monthly data. This process is done by calculating the monthly mean data for each month.

The next step is to understand and explore the dataset. Climate variables dataset contains time series data that mostly have patterns, either visible or invisible. To decompose such patterns, time series analysis is applied to find the seasonality and trend of the dataset [Liu et al., 2024]. The decomposition includes multiplicative model and the frequency every 12 month for each climate variables.

The relationship between climate variables is determined by calculating the Pearson correlation coefficient. The relationship between two time series data is represented by a range value from -1.0 to +1.0 . The coefficient close to -1.0 implying that two time series have opposite relationship, the values in a dataset decreasing meanwhile in another dataset increasing. Otherwise, the coefficient close to +1.0 indicating that the two data are positively related, the values in a dataset increasing as in another dataset. Meanwhile, the coefficient is equal to 0 meaning that there is no relationship between the datasets. The formula to calculate the correlation coefficient for a sample is shown in the Equation 2 below [Teng and Chen, 2024],

$$r_{\psi\phi} = \frac{\sum_{i=1}^n (\psi_i - \bar{\psi})(\phi_i - \bar{\phi})}{\sqrt{\sum_{i=1}^n (\psi_i - \bar{\psi})^2} \sqrt{\sum_{i=1}^n (\phi_i - \bar{\phi})^2}} \quad (2)$$

where:  $n$  is sample size,  $\psi$  and  $\phi$  are the two different datasets,  $i$  is the data indexing, and the symbols with bar such as  $\bar{\psi}$  are the mean of corresponding data set.

SVR is a widely recognized technique for categorizing data within two-dimensional spaces in across disciplines. It is capable of generating precise regression models for both linear and nonlinear regression problem. Basically, similar to ordinary regression technique, SVR algorithm construct a curve as function that fits to dataset. SVR also can be view as a model that fits data with specific error tolerance as thickness of a curve  $\epsilon$  such that the test data has minimum error [Liao et al, 2024; Zhang and O'Donnell, 2020]. The implementation of SVR in this paper use scikit-learn SVR application programming interface (API) [Chang and Lin, 2011].

The dataset is transformed to daily dataset over ten years, from 2013 to 2022. The dataset is separated to train and test dataset. The train dataset includes the mean climate variables from location 1 to location 2 in spanning years from 2013 to 2021. Similarly, the test dataset consists of the mean climate variables in the year of 2022. Then these two datasets are scaled with values from 0 to 1. The next step is to set the SVR model with free parameters consist of C, epsilon, and gamma which equal to 0.1, 0.01, and 0.01 respectively. Moreover, radial basis function kernel is also applied to the model. Next step fits the model with the train dataset. The trained model is employed to predict the test dataset and measure its performance. The performance of the model is computed using MSE.

## RESULTS AND DISCUSSIONS

Figure 2 represent the climate variables datasets containing wind speed, SST, total precipitation, and surface pressure of each location, the dataset spanning from 2013 to 2022. The wind speed dataset of each location is illustrated in Figure 2a. It can be seen that the location shows high peaks in wind speed are location 1. These peaks are above 8 m/s. The lowest wind speed of each location varies dominated by wind speed in location 1, 2, and 3. All of the locations show the peak patterns year by year. It occurs between May and October. Otherwise, the crest patterns occur between November and April. Figure 2b depicts the dataset of SST in each location. Overall, the lowest crest of the dataset is shown at location 2. These low points occur in between May and October and the high points of SST happen from November to April. From the dataset, the majority

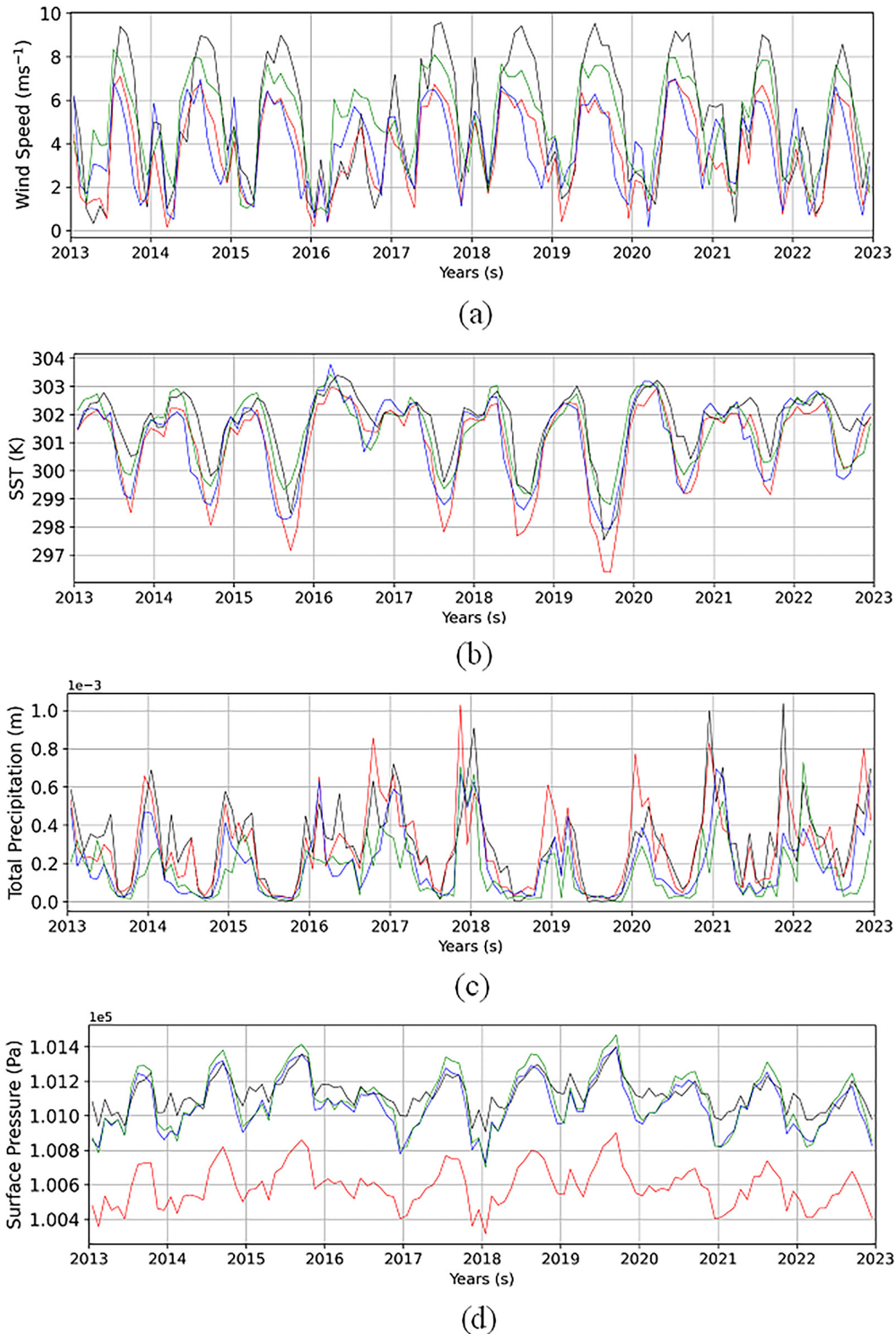


**Figure 2.** The dataset of (a) wind speed, (b) SST, (c) total precipitation, and (d) surface pressure of each location. Black, red, blue, and green lines indicate the dataset of location 1, 2, 3, and 4 respectively

low points of SST are at location 2. The total precipitation dataset is represented by Figure 2c. The y-axis of Figure 2c is presented in order of  $10^{-3}$ . The high precipitation points happen at location 1

and 2. These points according to the dataset mainly occur between November and March. Meanwhile the low points of total precipitation occur between June to October. Figure 2d illustrates the

surface pressure dataset of four locations. The y-axis in the figure represents the surface pressure in order  $10^5$ . As shown in the figure, there are two distinct separation which are the first consist of dataset of location 1, 3, and 4, and the other is the dataset of location 2. The later shows lower surface pressure than the other.

The trend of climate variables is shown in Figure 3. From these trends, it can be seen that all of the trends are correlated positively and negatively. For instance, Figure 3a depicts the trend of wind speed over ten years which is negatively correlated with the trend of SST in Figure 3b. Meanwhile, the trend of SST and total precipitation shows positive correlation (Figure 3b and 3c). Referring to Figure 3d, the trend of each location illustrates similar trend but difference for location 2 which is the surface pressure slightly lower than other three locations. This phenomenon can be exemplified by comparing figure 3b and 3d. In Figure 3b, it is apparent that the lowest SST occurs at location 2 (red line). The low

cold area corresponds to the low surface pressure in that area.

Figure 4 shows the seasonality of climate variables of each location. The wind speed seasonality illustrated in Figure 4a. there is two modes or peaks each year in the wind speed seasonality. The first peak of wind speed seasonality occurs in between May and July. The second peak is around January, in particular at location 3. In the other hand, the lowest seasonality is in between February and April. The high wind speed in southern Java waters has been investigated that conclude that the rise happened starting from May to August and the low wind speed occurs between February to April [Wirasatriya et al., 2020]. In Figure 4b, the seasonality of SST shows opposite pattern compared with seasonality of wind speed. The warm area arises in between January and March. Meanwhile, the low SST take place in between July and October. Based on previous research, the high SST starts from the end of December to April and the low SST occur from July

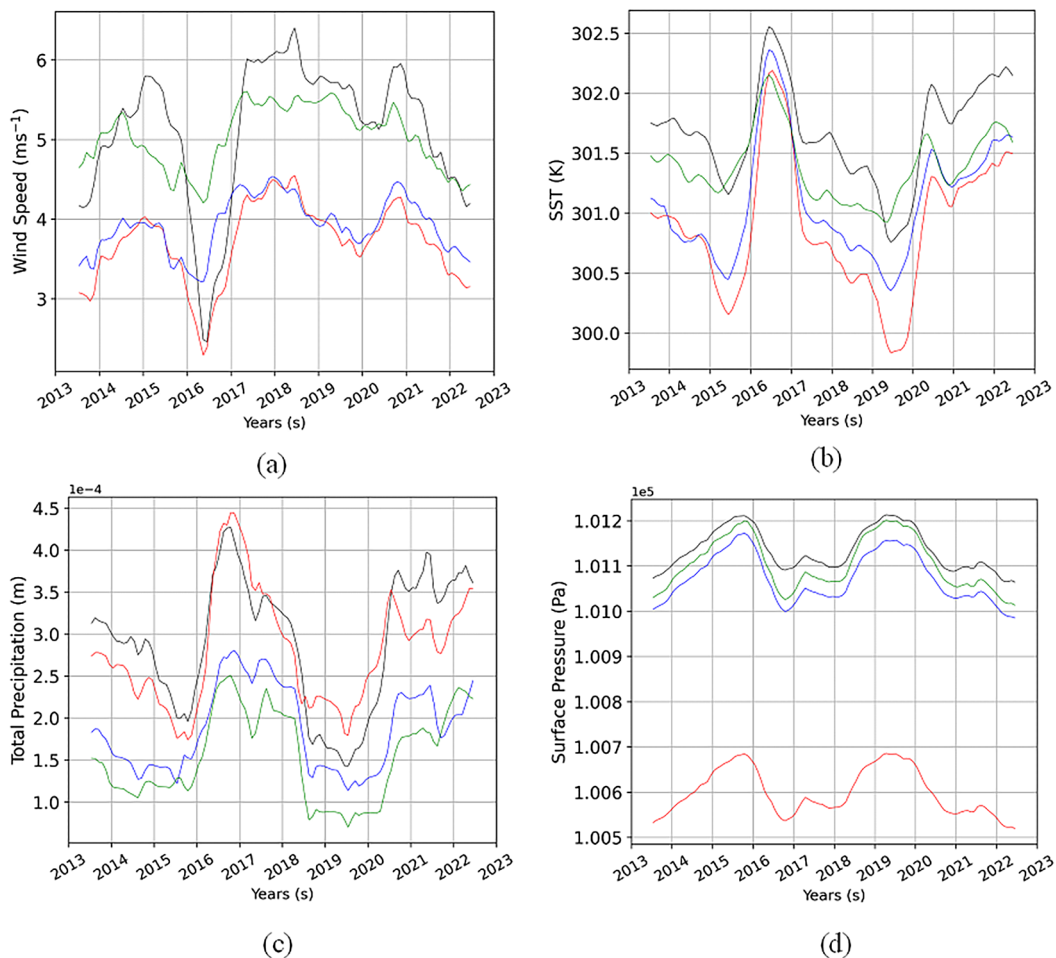


**Figure 3.** The trend of (a) wind speed, (b) SST, (c) total precipitation, and (d) surface pressure of each location. Black, red, blue, and green lines indicate the dataset of location 1, 2, 3, and 4 respectively

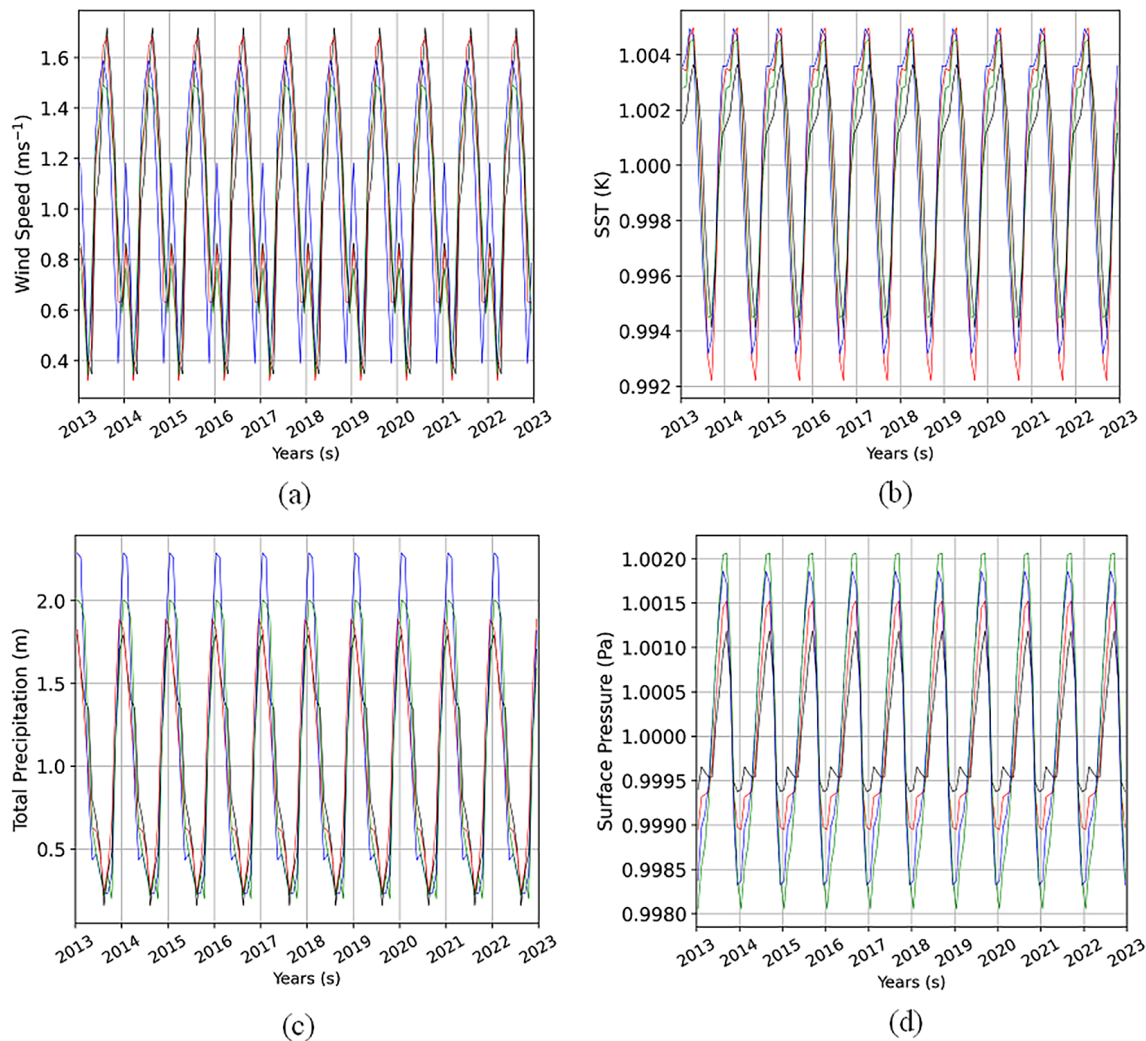


**Figure 4.** The seasonality of (a) wind speed, (b) SST, (c) total precipitation, and (d) surface pressure of each location. Black, red, blue, and green lines indicate the dataset of location 1, 2, 3, and 4 respectively

to September, the peak in August [Wirasatriya et al., 2020]. Figure 4c illustrates similar pattern to seasonality of SST. The Highest seasonality of total precipitation arises from January to February. The Lowest seasonality occurs in between September to November. The seasonality of surface pressure and wind speed almost shows identical pattern. Depicted by Figure 4d, the high seasonality of surface pressure is happened in between June and August. Meanwhile, the low seasonality is occurred in between December to February.

The relationship between climate variables is depicted by Figure 5, the darker the color showing negative correlation and the lighter the color showing positive correlation. In Figure 5, WS, SST, TP, and SP stand for wind speed, sea surface temperature, total precipitation, and surface pressure, respectively. Figure 5a demonstrate the correlation matrix of location 1. Wind speed

is positively correlated with surface pressure at 0.52. In the other hand, it is negatively correlated with SST at -0.7. Wind speed in location 1 also shows opposite correlation with total precipitation at -0.49. SST in location 1 has positive correlation with total precipitation at 0.51 and it has negative correlation with surface pressure at -0.67. Overall, these relationships between climate variables also illustrated similar recurrence at location 2, 3, and 4 but with difference value correlation constant.

From the previous studies, wind speed has positive correlation with surface pressure but negative correlation with SST [Mondal et al., 2022; Sofiati et al., 2020]. Moreover, SST has positive relationship with total precipitation [Nugroho, 2015]. Total precipitation has negative correlation with wind speed. This process is caused by low SST in particular during El Niño event that

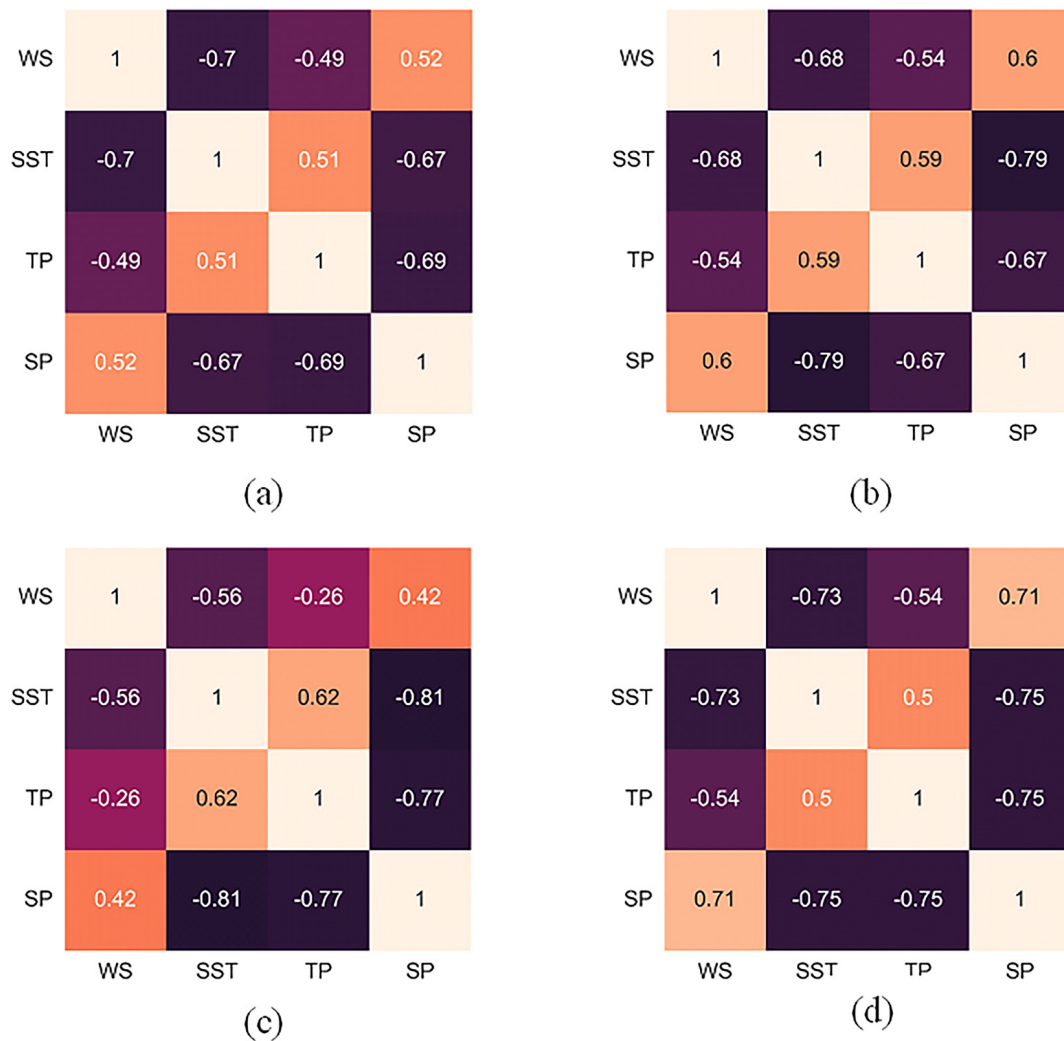


**Figure 5.** The correlation matrix between climate variables of location (a) 1, (b) 2, (c) 3, and (d) 4

caused low-level wind and pressure divergence which leads to rise the rainfall [Hendon, 2003].

The comparison between SVR model and actual dataset is shown in Figure 6. The prediction of the year of 2022 is compared with the test data or in this case the actual dataset. Figure 6a is the representation of model prediction result of wind speed. The predicted curve is smoother than the actual dataset. This smoothness is also shown in the Figure 6b of SST and Figure 6d of surface pressure. The smoothness behaviour depends on the value of regularization parameter gamma which sets to 0.01 as mentioned in the method section [Thomas et al., 2017]. Higher the gamma value leads to increase the model complexity and possibly produce an overfitted model. It can be seen that the models fit with all the climate variables. However, the performance of the model of total precipitation produces less accurate than other models as depicted in Figure 6c.

The performance of the models is calculated with a metric, MSE. The MSE values for each climate variables are depicted in Table 2. From the table, it can be seen that total precipitation has higher MSE value than other variables. It can also be seen that the prediction curve in Figure 6c is less accurate than other variables predicted curve. The lowest MSE value is happened to SST. This can be seen from Figure 6 that both actual dataset and predicted value of SST (Figure 6b) smoother and less fluctuation compared to other variables.

**Table 2.** The normalized of mean squared error of the SVR model

Climate variable	MSE
Wind speed	0.019
SST	0.002
Total precipitation	0.032
Surface pressure	0.014

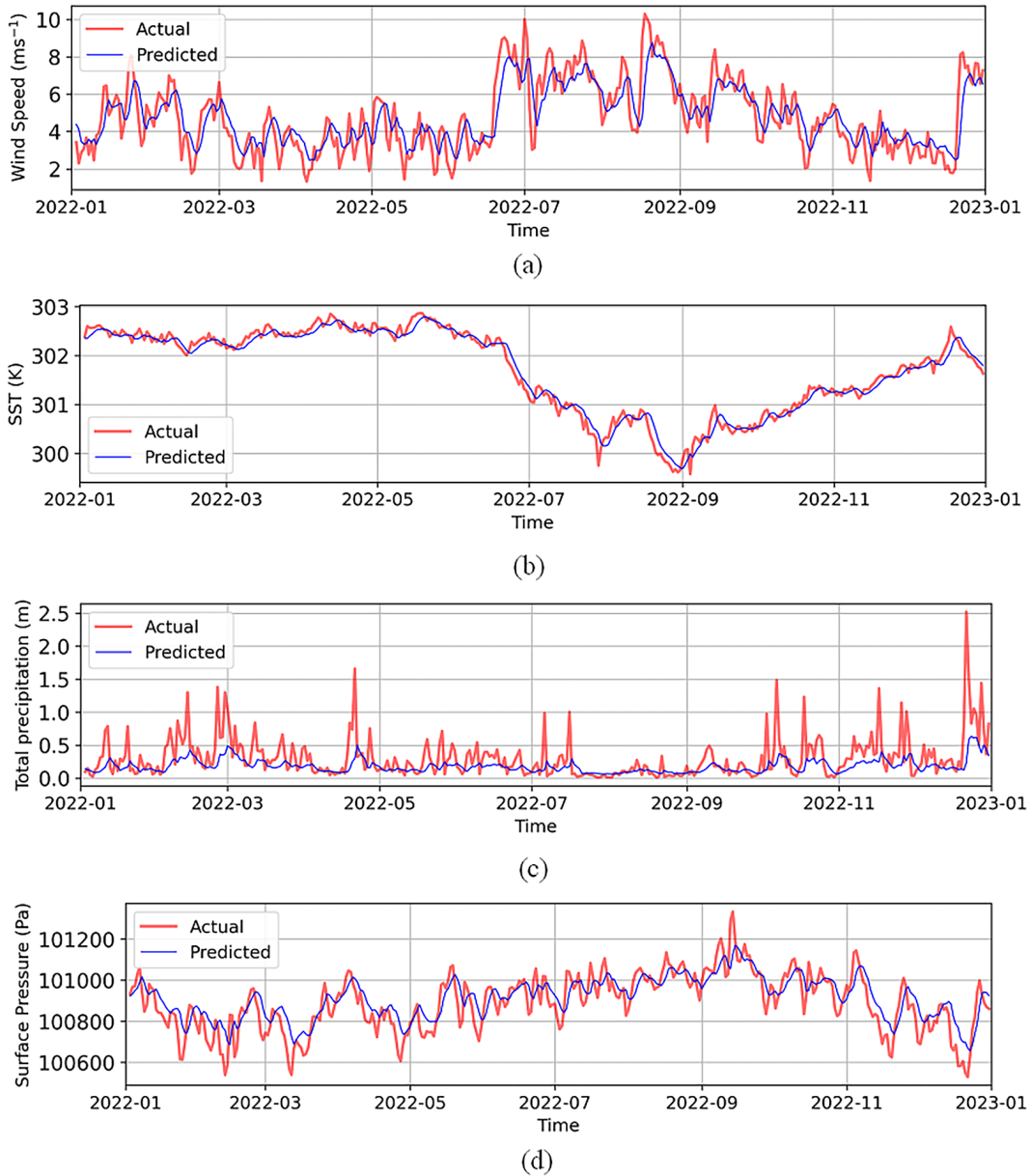


**Figure 6.** The SVR model prediction results compared with actual dataset of (a) wind speed, (b) SST, (c) total precipitation, and (d) surface pressure

**CONCLUSIONS**

Visually the relationship of each variable can be seen from the trend curve. Unfortunately, this visual approach does not explain exactly about the relationship. The relationships of each climate variables in the Southern Java Waters are computed using correlation matrix. In the matrix, wind speed and SST show negative correlation meaning that the higher the wind speed the lower the SST value. Also, the matrix illustrates positive relationship between wind speed and surface pressure. Meanwhile, SST and total precipitation correspond positively. This research builds model for predicting climate

variables in the future. The model performance is determined using MSE, the lower the MSE value, the better the model. The highest MSE value occurs for total precipitation model. On the other hand, the lowest MSE value occurs for SST. These behaviors happen because of the nature of the dataset. The SST dataset less fluctuates than other climate variables dataset.

**Acknowledgements**

The authors would like to thank Department of Oceanography, Diponegoro University, Indonesia for providing computing resources.

## REFERENCES

- Budiman, A.S., Bengen, D.G., Nurjaya, I.W., Arifin, Z. and Ismail, M.F.A. (2022). A comparison of the three upwelling indices in the South Java sea shelf. *CMU J. Nat. Sci.*, 21(3), p.e2022044.
- Chang, C.C. and Lin, C.J. (2011). LIBSVM: a library for support vector machines. *ACM transactions on intelligent systems and technology (TIST)*, 2(3), 1–27.
- Dash, R.K., Nguyen, T.N., Cengiz, K. and Sharma, A. (2023). Fine-tuned support vector regression model for stock predictions. *Neural Computing and Applications*, 35(32), 23295–23309.
- Docquier, D., Vannitsem, S. and Bellucci, A. (2023). The rate of information transfer as a measure of ocean–atmosphere interactions. *Earth System Dynamics*, 14(3), 577–591.
- Drucker, H., Burges, C.J., Kaufman, L., Smola, A. and Vapnik, V. (1996). Support vector regression machines. *Advances in neural information processing systems*, 9.
- Fanin, T. and Van Der Werf, G.R. (2017). Precipitation–fire linkages in Indonesia (1997–2015). *Bio-geosciences*, 14(18), 3995–4008.
- Feng, Z.K., Niu, W.J., Tang, Z.Y., Jiang, Z.Q., Xu, Y., Liu, Y. and Zhang, H.R. (2020). Monthly runoff time series prediction by variational mode decomposition and support vector machine based on quantum-behaved particle swarm optimization. *Journal of Hydrology*, 583, 124627.
- Hadi, S., Ningsih, N.S., Baskoro, M.S., Wirasatriya, A. and Kuswardani, A.R. (2020), July. The classification of upwelling indicators base on sea surface temperature, chlorophyll-a and upwelling index, the case study in Southern Java to Timor Waters. In *IOP Conference Series: Earth and Environmental Science* 530(1), 012020. IOP Publishing.
- Harris, C.R., Millman, K.J., Van Der Walt, S.J., Gommers, R., Virtanen, P., Cournapeau, D., Wieser, E., Taylor, J., Berg, S., Smith, N.J. and Kern, R. (2020). Array programming with NumPy. *Nature*, 585(7825), 357–362.
- Hendon, H.H. (2003). Indonesian rainfall variability: Impacts of ENSO and local air–sea interaction. *Journal of Climate*, 16(11), 1775–1790.
- Hersbach, H., Bell, B., Berrisford, P., Hirahara, S., Horányi, A., Muñoz-Sabater, J., Nicolas, J., Peubey, C., Radu, R., Schepers, D. and Simmons, A. (2020). The ERA5 global reanalysis. *Quarterly Journal of the Royal Meteorological Society*, 146(730), 999–2049.
- Horii, T., Siswanto, E., Iskandar, I., Ueki, I. and Ando, K. (2022). Can coastal upwelling trigger a climate mode? a study on intraseasonal-scale coastal upwelling off java and the indian ocean dipole. *Geophysical Research Letters*, 49(15), p.e2022GL098733.
- Hoyer, S. & Hamman, J. (2017). Xarray: N-D labeled Arrays and Datasets in Python. *Journal of Open Research Software*, 5(1), 10.
- Hunter, J.D. (2007). Matplotlib: A 2D Graphics Environment. *Computing in Science & Engineering*, 9(3), 90–95.
- Iskandar, M.R., Ismail, M.F.A., Arifin, T. and Chandra, H. (2021). Marine heatwaves of sea surface temperature off south Java. *Heliyon*, 7(12).
- Iwabuchi, B.L. and Gosselin, L. A. (2019). Long-term trends and regional variability in extreme temperature and salinity conditions experienced by coastal marine organisms on Vancouver Island, Canada. *Bulletin of Marine Science*, 95(3), 337–354.
- Kuswanto, H. and Ningtyas, N.N.A., (2016), October. Composite maps of surface pressure and geopotential to predict extreme high temperature in Surabaya. In *2016 12th International Conference on Mathematics, Statistics, and Their Applications (ICMSA)* 139–143. IEEE.
- Liao, Z., Dai, S. and Kuosmanen, T. (2024). Convex support vector regression. *European Journal of Operational Research*, 313(3), 858–870.
- Liu, F., Song, F. and Luo, Y., (2024). Human-induced intensified seasonal cycle of sea surface temperature. *Nature Communications*, 15(1), 3948.
- Met Office, U.K. (2010). *Cartopy: A cartographic python library with a matplotlib interface*. Exeter, Devon.
- Mondal, S., Lee, M.A., Wang, Y.C. and Semedi, B., (2022). Long-term variation of sea surface temperature in relation to sea level pressure and surface wind speed in southern Indian Ocean. *Journal of Marine Science and Technology*, 29(6), 784–793.
- Muhammad, F.R. and Lubis, S.W. (2022). Impacts of the boreal summer intraseasonal oscillation on precipitation extremes in Indonesia. *International Journal of Climatology*, 43(PNNL-SA-177965).
- Mutaqin, B.W. and Ningsih, R.L. (2023). Tidal characteristics in the Southern Waters of Java-Indonesia. *Jurnal Geografi*, 15(2), 154–164.
- Nugroho, B.D.A. (2015). Relationships between Sea Surface Temperature (SST) and rainfall distribution pattern in South-Central Java, Indonesia. *The Indonesian Journal of Geography*, 47(1), 20.
- Nurlatifah, A., Susanti, I. and Suhermat, M. (2021). Variability and trend of sea level in southern waters of Java, Indonesia. *Journal of Southern Hemisphere Earth Systems Science*, 71(3), 272–283.
- Parbat, D. and Chakraborty, M. (2020). A python based support vector regression model for prediction of COVID19 cases in India. *Chaos, Solitons & Fractals*, 138, 109942.
- Ramadhan, R., Marzuki, M., Suryanto, W., Sholihun, S., Yusnaini, H., Muharsyah, R. and Hanif, M. (2022). Trends in rainfall and hydrometeorological disasters

- in new capital city of Indonesia from long-term satellite-based precipitation products. *Remote Sensing Applications: Society and Environment*, 28, 100827.
28. Scrosati, R.A. (2020). Upwelling spike and marked SST drop after the arrival of cyclone Dorian to the Atlantic Canadian coast. *Journal of Sea Research*, 159, 101888.
29. Singh, V.K. and Roxy, M.K. (2022). A review of ocean-atmosphere interactions during tropical cyclones in the north Indian Ocean. *Earth-Science Reviews*, 226, 103967.
30. Sofiati, I. and Putranto, M.F. (2020), September. The analysis of tropical cyclones that occurred in the southern sea of Java during the period 2004-2019 and their effects on sea-atmospheric conditions. In *IOP Conference Series: Earth and Environmental Science* 572, 1, 012032). IOP Publishing.
31. Sofiati, I., Yulihastin, E., Suaydhi, S. and Putranto, M.F. (2020). Meridional variations of sea surface temperature and wind over southern sea of Java and its surroundings. *Journal of Physics and Its Applications*, 3(1), 129–135.
32. Teng, T.P. and Chen, W.J. (2024). Using Pearson correlation coefficient as a performance indicator in the compensation algorithm of asynchronous temperature-humidity sensor pair. *Case Studies in Thermal Engineering*, 53, 103924.
33. Thomas, S., Pillai, G.N. and Pal, K. (2017). Prediction of peak ground acceleration using  $\epsilon$ -SVR,  $\nu$ -SVR and Ls-SVR algorithm. *Geomatics, Natural Hazards and Risk*, 8(2), 177–193.
34. Vapnik, V. (2013). The nature of statistical learning theory. Springer science & business media.
35. Wang, C. (2019). Three-ocean interactions and climate variability: a review and perspective. *Climate Dynamics*, 53(7–8), 5119–5136.
36. Wen, C., Wang, Z., Wang, J., Li, H., Shi, X., Gao, W. and Huang, H. (2023). Variation of the coastal upwelling off South Java and their impact on local fishery resources. *Journal of Oceanology and Limnology*, 1–16.
37. Wijaya, Y.J., Wisha, U.J., Rejeki, H.A. and Ismunarti, D.H. (2023). Variability of the South Java Current from 1993 to 2021, and its relationship to ENSO and IOD events. *Asia-Pacific Journal of Atmospheric Sciences*, 1–15.
38. Wirasatriya, A., Setiawan, J.D., Sugianto, D.N., Rosyadi, I.A., Haryadi, H., Winarso, G., Setiawan, R.Y. and Susanto, R.D. (2020). Ekman dynamics variability along the southern coast of Java revealed by satellite data. *International Journal of Remote Sensing*, 41(21), 8475–8496.
39. Zhang, F. and O'Donnell, L.J. (2020). *Support vector regression*. In Machine learning. Academic Press.